Toward order-by-order calculations of the nuclear and neutron matter equations of state in chiral effective field theory

F. Sammarruca, L. Coraggio, J. W. Holt, N. Itaco, R. Machleidt, and L. E. Marcucci

Towards order-by-order calculations of the nuclear and neutron matter equations of state in chiral effective field theory

F. Sammarruca,[1] L. Coraggio,[2] J. W. Holt,[3] N. Itaco,[2, 4] R. Machleidt,[1] and L. E. Marcucci[5, 6]

[1]*Department of Physics, University of Idaho, Moscow, ID 83844, USA*
[2]*Istituto Nazionale di Fisica Nucleare,*
Complesso Universitario di Monte S. Angelo, Via Cintia - I-80126 Napoli, Italy
[3]*Department of Physics, University of Washington, Seattle, WA 98195, USA*
[4]*Dipartimento di Fisica, Università di Napoli Federico II,*
Complesso Universitario di Monte S. Angelo, Via Cintia - I-80126 Napoli, Italy
[5]*Dipartimento di Fisica "Enrico Fermi", Università di Pisa, Largo Bruno Pontecorvo 3 - I-56127 Pisa, Italy*
[6]*Istituto Nazionale di Fisica Nucleare, Sezione di Pisa,*
Largo Bruno Pontecorvo 3 - I-56127 Pisa, Italy

We calculate the nuclear and neutron matter equations of state from microscopic nuclear forces at different orders in chiral effective field theory and with varying momentum-space cutoff scales. We focus attention on how the order-by-order convergence depends on the choice of resolution scale and the implications for theoretical uncertainty estimates on the isospin asymmetry energy. Specifically we study the equations of state using consistent NLO and N^2LO (next-to-next-to-leading order) chiral potentials where the low-energy constants c_D and c_E associated with contact vertices in the N^2LO chiral three-nucleon force are fitted to reproduce the binding energies of ^3H and ^3He as well as the beta-decay lifetime of ^3H. At these low orders in the chiral expansion there is little sign of convergence, while an exploratory study employing the N^3LO two-nucleon force together with the N^2LO three-nucleon force give first indications for (slow) convergence with low-cutoff potentials and poor convergence with higher-cutoff potentials. The consistent NLO and N^2LO potentials described in the present work provide the basis for estimating theoretical uncertainties associated with the order-by-order convergence of nuclear many-body calculations in chiral effective field theory.

I. INTRODUCTION

The equation of state (EoS) of highly neutron-rich matter is important for understanding wide ranging questions in contemporary nuclear structure physics, from the structure of rare isotopes (e.g., the thickness of neutron skins) to the properties of neutron stars. A quantity of central importance in many of these phenomena is the density-dependent nuclear symmetry energy, arising as the difference between the energy per particle of symmetric nuclear matter and pure neutron matter at a given density.

In astrophysical contexts, the EoS of neutron-rich matter is required over many orders of magnitude in the nuclear density, potentially up to ten times that of saturated nuclear matter. In principle, both one-boson-exchange as well as Dirac-Brueckner-Hartree-Fock (DBHF) calculations can access the high-density regime of the EoS. However, boson-exchange models (see, for instance, Ref. [1]) typically employ three-nucleon forces (3NFs) with little connection to the associated nucleon-nucleon (NN) force. For instance, large 3NF contributions arise from Δ-isobar intermediate states, whereas explicit Δ isobars are missing from the NN part. Relativistic approaches to the nuclear matter problem have been centered around the DBHF scheme [2]. The main strength of this framework is in its ability to account for an important class of 3NFs, namely virtual nucleon-antinucleon excitations, that lead to nuclear matter saturation close to the empirical density and energy [3].

Nowadays, microscopic nuclear many-body theory typically starts from the low-energy realization of QCD, chiral effective field theory [4, 5], and fits unresolved nuclear dynamics at short distances to the properties of two- and few-nucleon systems alone. The resulting potentials are then used to make predictions in nuclear many-body systems. The chiral effective field theory approach to nuclear and neutron matter has succeeded in producing realistic equations of state only with the inclusion of repulsive 3NFs arising at order N^2LO (next-to-next-to-leading order) in the chiral power counting [6–9]. In chiral effective field theory, the dominant two-pion-exchange component of this 3NF, with associated $c_{1,3,4}$ low-energy constants, is constructed consistently with the N^2LO two-body force. Many-body perturbation theory with low-momentum chiral nuclear forces [8] has been shown to reproduce qualitatively the saturation behavior found with renormalization-group-evolved two-body forces with refit low-energy constants in the 3NF sector [10, 11]. However, all low-momentum interactions are limited in calculations of the EoS to densities where the characteristic momentum scale (on the order of the Fermi momentum) is below the scale set by the momentum-space cutoff Λ in the NN potential regulating function, which for chiral NN forces typically has the form:

$$f(p', p) = \exp[-(p'/\Lambda)^{2n} - (p/\Lambda)^{2n}] \, , \tag{1}$$

where $\Lambda \lesssim 500\,\mathrm{MeV}$ is associated with the onset of favorable perturbative properties. Nonperturbative methods for computing the EoS with chiral nuclear forces are under active investigation [12–16] and may allow for higher values of the cutoff Λ (but still remaining below the chiral breakdown scale of about 1 GeV). Furthermore, concerning the range of densities which can be reliably accessed, we note that the Fermi momentum must be lower than the cutoff scale, regardless of the nature (perturbative or nonperturbative) of the many-body calculations. Although designed to reproduce similar NN scattering phase shifts, NN potentials with different regulator functions will yield different predictions in the nuclear many-body problem due to their different off-shell behavior. On the other hand, appropriate re-adjustment of the low-energy constants that appear in the nuclear many-body forces is expected to reduce the dependence on the regulator function [6].

Estimates of theoretical uncertainties [17] for calculations of the equation of state have largely focused on varying the low-energy constants and resolution scale at which nuclear dynamics are probed [6–8, 10–12]. In the present work we lay the foundation for order-by-order calculations of nuclear many-body systems by presenting consistent NLO and N^{2}LO chiral nuclear forces whose relevant short-range three-body forces are fit to $A = 3$ binding energies and the lifetime of the triton. We then assess the accuracy with which infinite nuclear matter properties and the isospin asymmetry energy can be predicted from order-by-order calculations in chiral effective field theory. Identifying the dominant sources of uncertainty in nuclear many-body calculations is an important open problem, especially as more stringent constraints on the EoS of neutron-rich matter and its density dependence are becoming available [18]. In computing the EoS, we employ the nonperturbative particle-particle ladder approximation, which re-sums an important class of diagrams accounting for Pauli-blocking in the medium.

We will employ NN potentials at NLO, N^{2}LO and N^{3}LO in the chiral expansion at resolution scales in the range $450\,\mathrm{MeV} \leq \Lambda \leq 600\,\mathrm{MeV}$ (for a recent review, see Ref. [20]). Note that we omit discussion of leading order (LO) chiral potentials, which are very crude and substantially less quantitative than interactions from sixty years ago, such as the Gammel-Thaler potential [19]. Thus, predictions at LO are not expected to meaningfully add to the discussion. Beyond NLO we include the leading chiral 3NF, whose low-energy constants are fitted to reproduce the binding energies of ^{3}H and ^{3}He as well as the beta-decay lifetime of ^{3}H [21]. Definite conclusions on convergence will be limited to the third order (N^{2}LO) in the chiral power counting, where fully consistent two- and three-nucleon forces are currently available. Similar studies, limited to pure neutron matter at and below the nuclear saturation density, have been performed in Ref. [12] up to N^{2}LO with two-body forces alone and in Ref. [7] for N^{2}LO and N^{3}LO chiral nuclear forces.

The paper is organized as follows. In Section II, we will describe detailed features of the NLO, N^{2}LO and N^{3}LO chiral NN potentials employed in the present work, together with consistent N^{2}LO three-nucleon forces when appropriate. In Section III we outline the calculations of the energy per particle of symmetric nuclear matter and pure neutron matter in the particle-particle ladder approximation employing chiral nuclear forces at different chiral orders and resolution scales. Results for the EoS and the nuclear symmetry energy up to a density of $\rho \simeq 0.3\,\mathrm{fm}^{-3}$ are presented. We end with a summary and conclusions.

II. DESCRIPTION OF THE CALCULATIONS

A. The two-nucleon potentials

In the present investigation we consider NN potentials at order $(q/\Lambda_\chi)^2$, $(q/\Lambda_\chi)^3$ and $(q/\Lambda_\chi)^4$ in the chiral power counting, where q denotes the small scale set by external nucleon momenta or the pion mass and Λ_χ is the chiral symmetry breaking scale. Chiral NN potentials at NLO and N^{2}LO, corresponding to $(q/\Lambda_\chi)^2$ and $(q/\Lambda_\chi)^3$, have been constructed previously in Ref. [22] for cutoffs ranging from $\Lambda = 450$ MeV to about 800 MeV. With varying chiral order and cutoff scale, the low-energy constants in the two-nucleon sector are refitted to elastic NN scattering phase shifts and properties of the deuteron. The low-energy constants $c_{1,3,4}$ associated with the $\pi\pi NN$ contact couplings of the $\mathcal{L}_{\pi N}^{(2)}$ chiral Lagrangian are given in Table I. We note that the c_i can be extracted from πN or NN scattering data. The potentials we use here [20, 23] follow the second path. At N^{2}LO, taking the range determined in πN analyses as a starting point, values were chosen to best reproduce NN data at that order, see Table 2 of Ref. [20]. At N^{3}LO, high-precision required a stronger adjustment of c_4 depending on the regulator function and cutoff. The fitting procedure is discussed in Ref. [20], where it is noted that the larger value for c_4 has, overall, a very small impact but lowers the $^3F_2$ phase shift for a better agreement with the phase shift analysis.

In Ref. [22], it was found that the two-body scattering phase shifts can be described well at NLO up to a laboratory energy of about 100 MeV, while the N^{2}LO potential fits the data up to 200 MeV. Interestingly, in the latter case the χ^2/datum was found to be essentially cutoff independent for variations of Λ between 450 and approximately 800 MeV. Finally, we also use NN potentials constructed at next-to-next-to-next-to-leading order (N^{3}LO) [20, 23], with

NLO	Λ (MeV)	n	c_1	c_3	c_4
	450	2			
	500	2			
	600	2			
N^2LO	Λ (MeV)	n	c_1	c_3	c_4
	450	3	-0.81	-3.40	3.40
	500	3	-0.81	-3.40	3.40
	600	3	-0.81	-3.40	3.40
N^3LO	Λ (MeV)	n	c_1	c_3	c_4
	450	3	-0.81	-3.40	3.40
	500	2	-0.81	-3.20	5.40
	600	2	-0.81	-3.20	5.40

TABLE I: Values of n and low-energy constants of the dimension-two πN Lagrangian, $c_{1,3,4}$, at each order and for each type of cutoff in the regulator function given in Eq. (1). None of the c_i's appears at NLO. The low-energy constants are given in units of GeV^{-1}.
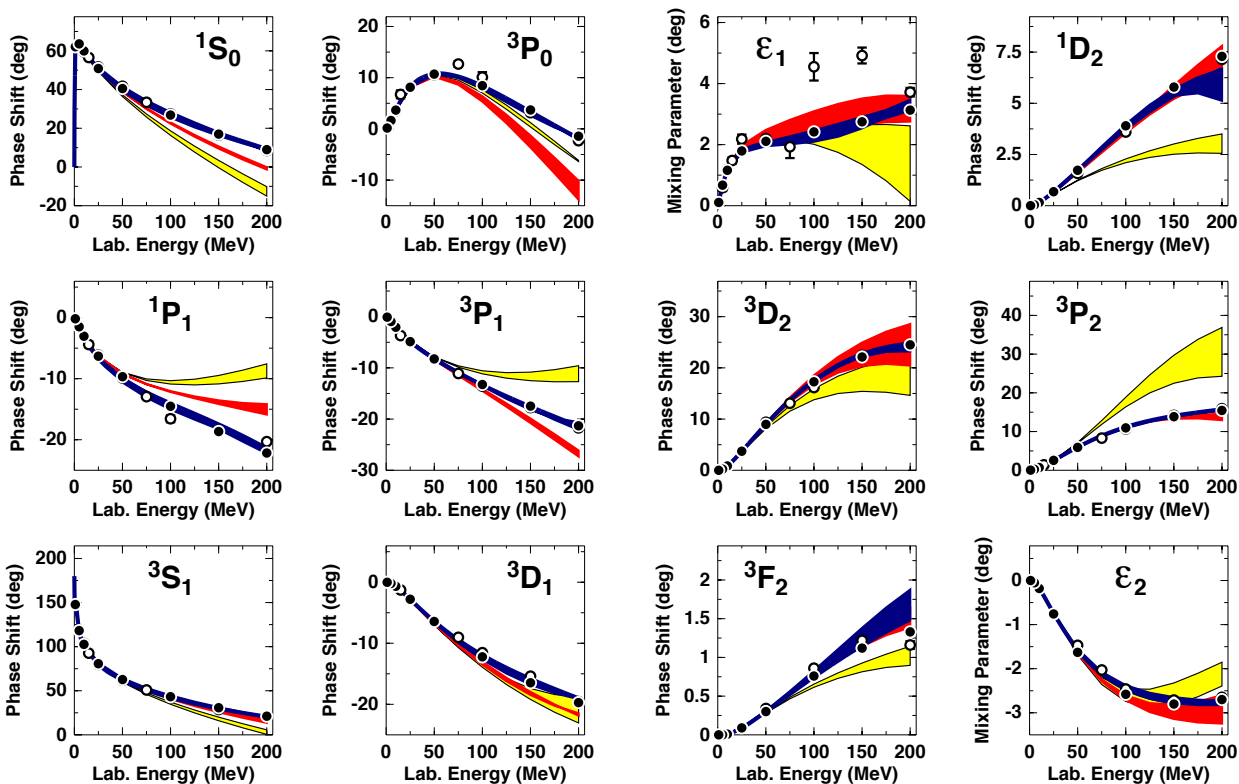

FIG. 1: (Color online) Phase shifts for some selected NN partial waves. The yellow, red, and blue bands show the variations of the predictions with changing cutoffs between 450 and 600 at NLO, N^2LO, and N^3LO, respectively.

low-energy constants $c_{1,3,4}$ as displayed in Table I. However, at N^3LO, NN potentials with cutoffs up to 800 MeV are not available. Therefore, in the present study, we limit the cutoff range to 450-600 MeV.

Before proceeding to the nuclear and neutron matter calculations, we demonstrate the dependence of NN scattering phase shifts on the chiral order and on the choice of the cutoff scale in the regulating function Eq. (1). Results are shown in Fig. 1, where the yellow, red and blue bands indicate the NLO, N^2LO, and N^3LO results, respectively, obtained from varying the cutoff between 450 and 600 MeV. Although N^2LO calculations can achieve sufficient accuracy in selected partial wave channels up to $E_{\text{lab}} = 200\,\text{MeV}$, only the N^3LO interactions achieve the level of high-precision potentials, characterized by a $\chi^2/\text{datum} \sim 1$.
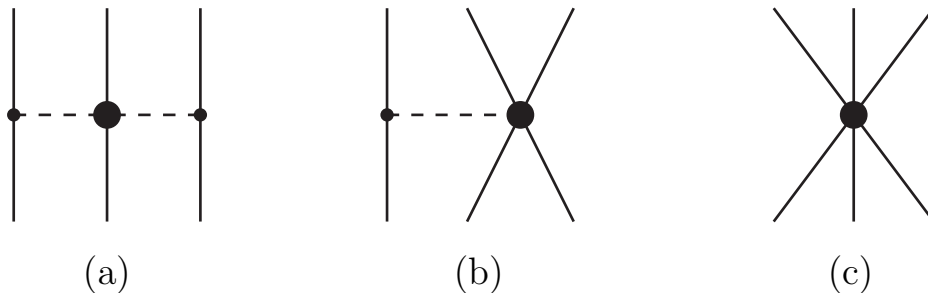
FIG. 2: Diagrams of the 3NF at N^{2}LO. See text for more details.

At the two-body level each time the chiral order is increased, the NN contact terms and/or the two-pion-exchange contributions proportional to the low-energy constants $c_{1,3,4}$ are refitted. We recall that at N^{2}LO no new NN contact terms are generated, and therefore improved cutoff independence in the NN phase shifts (compare the yellow and red bands in Fig. 1) is due to changes in the two-pion-exchange contributions. At N^{2}LO, subleading $\pi\pi NN$ vertices enter into the chiral NN potential. These terms encode the important physics of correlated two-pion-exchange and the excitation of intermediate $\Delta(1232)$ isobar states. Thus, only at this order is it possible to obtain a realistic description of the NN interaction at intermediate-range, traditionally generated through the exchange of a fictitious σ meson of intermediate mass. At N^{3}LO in the chiral power counting, the 15 additional NN contact terms (bringing the total to 24 at N^{3}LO) result in a much improved description of NN scattering phase shifts.

We observe that the calculated phase shifts are in most cases not renormalization group invariant, though with increasing chiral order the dependence on the cutoff scale is generally reduced. The standard Weinberg's power counting in which contributions to the NN potential are computed perturbatively with loop integrals renormalized through counterterms, is employed in the present work. Weinberg's scheme implicitly assumes that the counterterms introduced to renormalize the perturbative potential are sufficient to also renormalize its nonperturbative resummation, e.g., in the Lippmann-Schwinger equation for computing phase shifts. Kaplan *et al.* [41], however, pointed out the presence of problems with this assumption, which stimulated intense discussion in the literature [42]. In particular, Nogga *et al.* [43] performed a systematic investigation of Weinberg's power counting at lowest order and proposed a modified scheme in which contact terms from NLO are promoted to LO to take care of the cutoff dependence in $^3P_0$ and $^3P_2$, and from N^{3}LO to LO to address the same problem in $^3D_2$. On the other hand, the consistency problem of Weinberg's power counting appears to be minimal when implemented together with finite-cutoff regularization below the high-energy scale of the effective field theory. It has been shown [22] that, at a given order, cutoff ranges can be identified where the χ^2 of the fit to the NN data is essentially flat (that is, cutoff independent). In other words, order-by-order renormalization can be accomplished successfully with finite cutoffs in Weinberg's power counting, and errors associated with variations in the momentum-space cutoff (a regularization prescription that does not respect chiral symmetry) are typically of the same order as the error expected from the truncated chiral expansion.

B. Chiral three-body interactions

Three-nucleon forces make their appearance at third order in the chiral power counting. They are expressed as the sum of three contributions: the long-range two-pion-exchange part with $\pi\pi NN$ vertex proportional to the low-energy constants c_1, c_3, c_4, the medium-range one-pion exchange diagram proportional to the low-energy constant c_D, and finally the short-range contact term proportional to c_E. The corresponding diagrams are shown in Fig. 2, labeled as (a), (b), (c), respectively.

Thr natural framework to include 3NFs in the particle-particle ladder approximation to the energy per particle in homogeneous nuclear matter would be the Bethe-Faddeev equation. To facilitate this inclusion, we employ the density-dependent NN interaction derived in Refs. [24, 25] from the N^{2}LO chiral three-body force. This effective interaction is obtained by summing one particle line over the occupied states in the Fermi sea. Neglecting small contributions [26] from terms depending on the center-of-mass momentum, the resulting NN interaction can be expressed in analytical form with operator structures identical to those of free-space NN interactions. For symmetric nuclear matter all three-body forces contribute, while for pure neutron matter only terms proportional to the low-energy constants c_1 and c_3 are nonvanishing [25, 26]. Previous studies (see e.g., Ref. [8]) have found that 3NF contributions to the energy per particle are dominant at the Hartree-Fock level. When three-body forces are approximated with a density-

N^{2}LO	Λ (MeV)	c_D	c_E
	450	-0.326	-0.149
	500	-0.165	-0.169
	600	0.456	-0.859
N^{3}LO	Λ (MeV)	c_D	c_E
	450	-0.24	-0.11
	500	0.0	-0.18
	600	-0.19	-0.83

TABLE II: Values of the c_D and c_E low-energy constants obtained using the N^{2}LO 3NF in conjunction with NN interactions of different orders, for several values of the cutoff Λ. These constants do not appear at NLO.

dependent NN interaction, certain topologies are missing at and beyond second order in perturbation theory. In the case of a pure contact interaction the additional topologies reduce the second-order contribution to the energy per particle by about 50% at saturation density [27], which corresponds in the present calculation to an uncertainty of $\Delta E/A \lesssim 1$ MeV at saturation density.

We fix the low-energy constants c_D and c_E that appear in the N^{2}LO 3NF within the three-nucleon sector. Specifically, we constrain them to reproduce binding energies of $A = 3$ nuclei together with the Gamow-Teller matrix element in tritium β-decay, following a well established procedure [21, 28–33]. The values of c_D and c_E are given in Table II for the different chiral orders and cutoff scales. We note that the values at N^{3}LO in Table II are extracted from Refs. [8, 21], while those at N^{2}LO have been computed in the present work. Although efforts are in progress to incorporate potentially important N^{3}LO 3NF contributions [34–36], both in the fitting procedure and in the neutron and nuclear matter equations of state presented in the following section, the current "N^{3}LO" study is limited to the inclusion of the N^{2}LO three-body force together with the N^{3}LO two-body force, an approximation that is commonly used in the literature but whose associated uncertainties have not been carefully analyzed. In Refs. [7, 38], calculations of the neutron matter energy per particle at N^{3}LO show a small effect (of about -0.5 MeV) at saturation density for the potentials of our purview [20]. The Hartree-Fock contributions to the energy per particle of symmetric nuclear matter from the N^{3}LO 3NF are attractive and on the order of 7 MeV at saturation density [7]. The inclusion of 3NFs at N^{3}LO, however, necessitates a refitting of the c_D and c_E low-energy constants, which has not yet been performed and would likely result in a smaller change to the total energy per particle at saturation density. Most recently, evidence has been reported [37] that sub-leading terms in the 3NF may provide important contributions to the triton binding energy, as well as indications that similar conclusions apply in symmetric nuclear matter.

In the case of the N^{2}LO NN interaction with Λ = 600 MeV, small charge-symmetry-breaking effects have emerged in the fitting procedure. This is visible in Fig. 3, where the c_D-c_E trajectories which reproduce the experimental ^{3}H and ^{3}He binding energies are displayed. Allowing for charge-symmetry breaking, the values for c_E are -0.833 and -0.885 for ^{3}H and ^{3}He, respectively. The value shown in Table II is the average of these two. The error in the $A = 3$ binding energies, when the average value of c_E is used, is ~ 40 keV. We do not know at present the origin of this (small) charge-symmetry breaking effect.

III. NUCLEAR AND NEUTRON MATTER CALCULATIONS: RESULTS AND DISCUSSION

In this section we present results for the symmetric nuclear matter and neutron matter equations of state employing the particle-particle ladder approximation with the NN and $3N$ forces described above. In the traditional hole-line expansion [44], the particle-particle ladder diagrams comprise the leading-order contributions. The next set of diagrams is comprised of the three hole-line contributions, which includes the third-order particle-hole (ph) diagram considered in Ref. [8]. The third-order hole-hole (hh) diagram (fourth order in the hole-line expansion) was found to give a negligible contribution to the energy per particle at normal density irrespective of the cutoff (see Table II and Table III of Ref. [8]). The ph diagram is relatively much larger, bringing in an uncertainty of about ± 1 MeV (accounting for cutoff dependence $\Lambda \simeq 400 - 500$ MeV) on the potential energy per particle at normal density.

It is insightful to compare these values with those from Refs. [45, 46]. In Ref. [45], the authors report on coupled-cluster calculations in symmetric nuclear matter including pp and hh diagrams (as well as an exact treatment of the Pauli operator). The overall effect, as seen from comparing the first and last entries in Table II of Ref. [45], is very small around saturation density, consistent with Table II in Ref. [8], and grows to 1.5 MeV at the highest Fermi momentum included in the study. Note that these calculations adopt the N^{3}LO potential (with Λ=500 MeV) and only two-nucleon forces. On the other hand, in Ref. [46] coupled-cluster calculations in nucleonic matter were performed

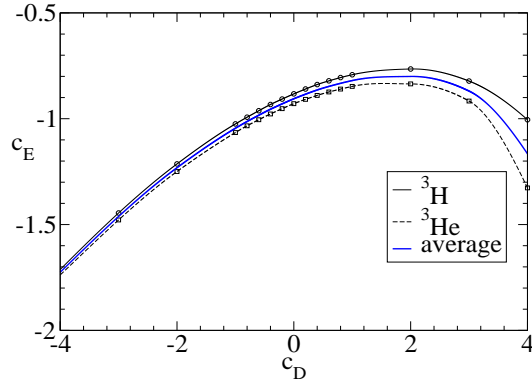FIG. 3: (Color online) c_E-c_D trajectories fitted to reproduce the experimental ^{3}H and ^{3}He binding energies in the case of the N^{2}LO NN interaction plus 3NF with $\Lambda = 600$ MeV. The average curve (in blue) is also displayed.

at N^{2}LO with two- and three-body forces and with the inclusion of selected triples clusters, namely correlations beyond pp and hh ladders. The effect of these contributions is found to be negligible in neutron matter and about 1 MeV per nucleon in symmetric matter in the density range under consideration [46]. Furthermore, it was shown in earlier studies [47] with meson-theoretic interactions (with larger momentum-space cutoffs) that when additional three hole-line contributions are taken into account, large cancellations occur which result in a small net effect on the energy per particle. This is especially the case when the continuous choice is adopted for the auxiliary potential [47]. In summary, we conclude that a realistic estimate of the impact of using a nonperturbative approach beyond pp correlations is about ± 1 MeV in nuclear matter around saturation density and much smaller in neutron matter. As we show below, such uncertainties are significantly smaller than those associated with variations in the cutoff scale.

Our results for the energy per particle as a function of the nuclear density are shown in Fig. 4 for symmetric nuclear matter. We note that the particle-particle ladder approximation employed in the present work is in good agreement with the perturbative results available at N^{3}LO from Ref. [8] including up to third-order pp diagrams. In the left panel of Fig. 4, the shaded bands in yellow and red represent the spread of our complete calculations conducted at NLO and N^{2}LO, respectively. The blue band is the result of a calculation that employs N^{3}LO NN potentials together with N^{2}LO 3NFs. In all cases shown, the cutoff is varied over the range 450-600 MeV. As noted before, the N^{3}LO 3NFs and 4NFs are at present omitted, and the resulting convergence pattern gives an estimate on the theoretical uncertainty of the calculation (and not of the chiral effective field theory expansion per se). On the right-hand side of the figure, the individual curves corresponding to each order and cutoff are displayed. We observe that at NLO the potentials constructed at lower cutoff scales do not exhibit saturation until very high densities. On the other hand, for the 600 MeV cutoff potential the $^1S_0$ partial wave (together with the $^3S_1$ partial wave) is sufficiently repulsive to enable saturation at a relatively smaller density. We observe that the convergence pattern for the low-cutoff ($\Lambda = 450 - 500$ MeV) potentials is significantly better than for the 600 MeV potential. Overall there is a large spread from cutoff variations both at NLO and N^{2}LO beyond nuclear matter saturation density. Moreover, the bands at these two orders do not overlap, suggesting that their width is not a suitable representation of the uncertainty. Although the (incomplete) N^{3}LO calculation reveals a strong reduction of the cutoff dependence, it is important to notice that an uncertainty of about 8 MeV remains at saturation density. While we do not expect much of a change in nuclear matter predictions from 4NFs [7, 39, 40], it is quite possible that the inclusion of N^{3}LO 3NFs might reduce either the cutoff dependence or improve the convergence pattern. This will be an interesting subject for future investigations.

The results for neutron matter are presented in Fig. 5, where the left and right panels have the same meaning as in Fig. 4. Note that the range of densities under consideration is smaller for neutron matter in order to keep the Fermi momentum below the cutoff in all cases. We see a large spread at NLO for the largest densities considered, whereas the band has only moderate size at the next order and remains small for our N^{3}LO calculation. Similar to what was observed in symmetric nuclear matter, the bands at NLO and N^{2}LO do not overlap in neutron matter. In addition the N^{3}LO band does not generally overlap with the N^{2}LO band. Therefore, the variation obtained by changing the cutoff does not seem to provide a reliable representation of the uncertainty at the given order. A better way to estimate such uncertainty is to consider the difference between the predictions at two consecutive orders.

In Fig. 6 we present the results for the symmetry energy E_{sym}, which is defined as the strength of the quadratic
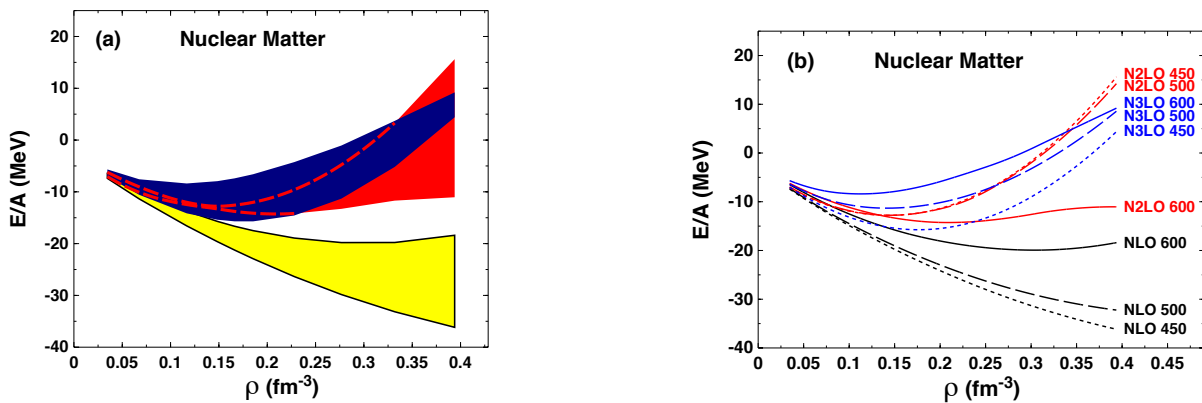
FIG. 4: (Color online) Energy/nucleon (E/A) in symmetric nuclear matter as a function of density, ρ. Left frame: The yellow and red bands represent the uncertainties in the predictions due to cutoff variations as obtained in complete calculations at NLO and N^{2}LO, respectively. The blue band is the result of a calculation employing N^{3}LO NN potentials together with N^{2}LO 3NFs. The dashed lines show the upper or lower limits of hidden bands. Right frame: predictions at the specified order and cutoff value.

term in an expansion of the energy per particle in asymmetric matter with respect to the asymmetry parameter α:

$$\bar{E}(\rho, \alpha) \approx \bar{E}(\rho, \alpha = 0) + E_{\text{sym}}\alpha^2 + \mathcal{O}(\alpha^4) \,, \tag{2}$$

where $\bar{E} = E/A$ is the energy per particle and $\alpha = (\rho_n - \rho_p)/(\rho_n + \rho_p)$. The nearly linear behavior of $\bar{E}(\rho, \alpha)$ with α^2 has been confirmed by many microscopic calculations (see for instance Ref. [48] and more recently Refs. [49, 50]). It justifies the common approximation of neglecting powers beyond α^2 in the expansion above and thus defining the symmetry energy as the difference between the energy per particle in neutron matter and symmetric nuclear matter.

It is well known that E_{sym} enters crucially in discussions of nuclear stability, and its density dependence around normal density strongly correlates with the neutron skin thickness of nuclei and the radius of (low-mass) neutron stars. As mentioned in Sec. I, systematic efforts are ongoing to set better empirical constraints on the symmetry energy, through both laboratory and astrophysical measurements. It is therefore important to have an understanding of the theoretical uncertainty affecting calculations of this quantity. The spread due to the change of the cutoff values in our NLO, N^{2}LO, and N^{3}LO calculations is represented by the three bands as before. As observed previously for symmetric matter, the spread due to cutoff variations remains large at N^{2}LO, with some minimal overlap with the NLO band. The N^{3}LO band reflects the large cutoff sensitivity previously observed in symmetric matter. Again, we conclude that the spread generated by changing the cutoff does not in general provide a reliable estimate of the theoretical uncertainty.

We close this section with some information on the density dependence of the symmetry energy, as revealed by the L parameter,

$$L = 3\rho_0 \Big(\frac{\partial E_{\text{sym}}}{\partial \rho}\Big)_{\rho_0} \,. \tag{3}$$

Namely, the L parameter reflects the slope of the symmetry energy at saturation density ρ_0. Our N^{3}LO result can be summarized as $L = 39.5^{+17.2}_{-13.6}$ MeV, whereas at N^{2}LO we find $L = 76.9^{+16.1}_{-31.2}$ MeV. We do not report a corresponding value at NLO, since, at that order, only the Λ=600 MeV case show some (late) saturating behavior. Constraints on L are not yet stringent, and can be quoted as $L = 70 \pm 25$ MeV [18].

IV. CONCLUSIONS

We have reported predictions for the energy per particle in symmetric nuclear matter and pure neutron matter, focusing on uncertainties related to order-by-order convergence. Compared to the consistent NLO and N^{2}LO results for the equations of state, which themselves exhibit relatively little overlap even for a large spread of momentum-space cutoffs $\Lambda = 450 - 600$ MeV, the results from employing N^{3}LO two-nucleon and N^{2}LO three-nucleon forces imply non-negligible uncertainties associated with missing higher-order terms in the chiral expansion. We find that the uncertainty associated with the cutoff variation is generally larger in symmetric nuclear matter than in pure neutron
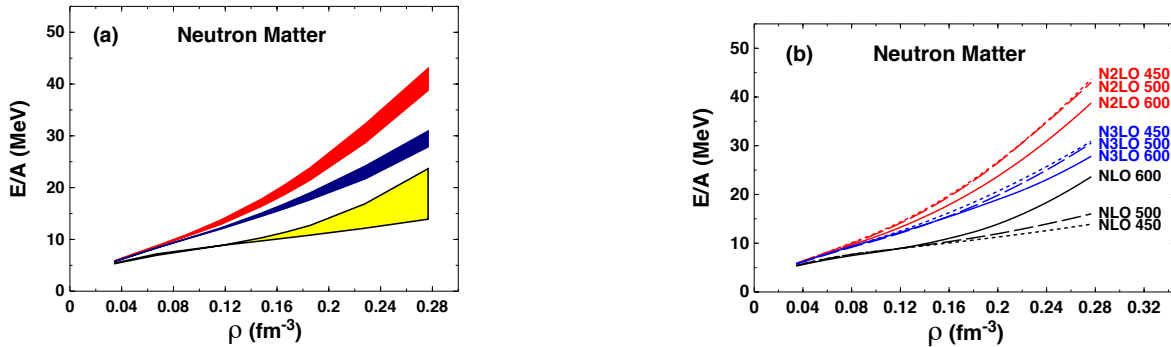
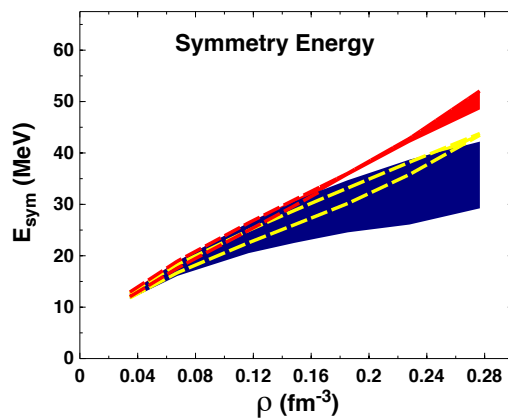FIG. 5: (Color online) As in Fig. 4 for pure neutron matter.

FIG. 6: (Color online) The symmetry energy, E_{sym}, as a function of density, ρ. Meaning of bands and dashed lines as in the right panel of Fig. 4.

matter, but in the latter case we find that the results from one chiral order to the next have little overlap. This suggests that further systematic studies of the order-by-order convergence should be performed, together with variations in the resolution scale and low-energy constants, to accurately estimate the complete theoretical uncertainties in chiral effective field theory predictions of nuclear many-body systems. The two- and three-body potentials considered in the present work can serve as a basis for such future uncertainty estimates.

Acknowledgments

[1] Z.H. Li, U. Lombardo, H.-J. Schulze, and W. Zuo, Phys. Rev. C **77**, 034316 (2008).
[2] F. Sammarruca, Int. J. Mod. Phys. E, **22**, 1330031 (2014), and references therein.
[3] F. Sammarruca, B. Chen, L. Coraggio, N. Itaco, and R. Machleidt, Phys. Rev. C **86**, 054317 (2012).
[4] S. Weinberg, Phys. Rev. **166**, 1568 (1968).
[5] S. Weinberg, Physica **96A**, 327 (1979).
[6] L. Coraggio, J. W. Holt, N. Itaco, R. Machleidt and F. Sammarruca, Phys. Rev. C **87**, 014322 (2013).
[7] T. Krüger, I. Tews , K. Hebeler, and A. Schwenk, Phys. Rev. C **88**, 025802 (2013).

[8] L. Coraggio, J. W. Holt, N. Itaco, R. Machleidt, L. E. Marcucci, and F. Sammarruca, Phys. Rev. C **89**, 044321 (2014).

[9] C. Wellenhofer, J. W. Holt, N. Kaiser and W. Weise, Phys. Rev. C **89**, 064009 (2014).

[10] S. K. Bogner, A. Schwenk, R. J. Furnstahl, and A. Nogga, Nucl. Phys. A **763**, 59 (2005).

[11] K. Hebeler, S. K. Bogner, R. J. Furnstahl, A. Nogga, and A. Schwenk, Phys. Rev. C **83**, 031301 (2011).

[12] A. Gezerlis, I. Tews, E. Epelbaum, S. Gandolfi, K. Hebeler, A. Nogga, and A. Schwenk, Phys. Rev. Lett. **111**, 032501 (2013).

[13] G. Hagen, T. Papenbrock, A. Ekström, K. A. Wendt, G. Baardsen, S. Gandolfi, M. Hjorth-Jensen and C. J. Horowitz, Phys. Rev. C **89**, 014319 (2014).

[14] A. Roggero, A. Mukherjee, and F. Pederiva, Phys. Rev. Lett. **112**, 221103 (2014).

[15] G. Wlazłowski, J. W. Holt, S. Moroz, A. Bulgac, and K. Roche, Phys. Rev. Lett. **113**, 182503 (2014).

[16] A. Carbone, A. Rios, and A. Polls, arXiv:1408.0717.

[17] R. J. Furnstahl, D. R. Phillips, and S. Wesolowski, J. Phys. G **42**, 034028 (2015).

[18] M.B. Tsang *et al.*, Phys. Rev. C **86**, 015803 (2012).

[19] J.L. Gammel, R.M. Thaler, Phys. Rev. **107**, 291 (1957).

[20] R. Machleidt and D.R. Entem, Phys. Rep. **503**, 1 (2011).

[21] L.E. Marcucci, A. Kievsky, S. Rosati, R. Schiavilla, and M. Viviani, Phys. Rev. Lett. **108**, 052502 (2012).

[22] E. Marji, A. Canul, Q. MacPherson, R. Winzer, Ch. Zeoli, D.R. Entem, and R. Machleidt, Phys. Rev. C **88**, 054002 (2013).

[23] D.R. Entem and R. Machleidt, Phys. Rev. C **68**, 041001 (2003).

[24] J. W. Holt, N. Kaiser, and W. Weise, Phys. Rev. C **79**, 054331 (2009).

[25] J. W. Holt, N. Kaiser, and W. Weise, Phys. Rev. C **81**, 024002 (2010).

[26] K. Hebeler and A. Schwenk, Phys. Rev. C **82**, 014314 (2010).

[27] N. Kaiser, Eur. Phys. J. A **48**, 58 (2012).

[28] A. Gardestig and D.R. Phillips, Phys. Rev. Lett. **96**, 232301 (2006).

[29] D. Gazit, S. Quaglioni, and P. Navratil, Phys. Rev. Lett **103**, 102502 (2009).

[30] M. Viviani, L. Girlanda, A. Kievsky, and L.E. Marcucci, Phys. Rev. Lett. **111**, 172302 (2013).

[31] M. Piarulli, L. Girlanda, L.E. Marcucci, S. Pastore, R. Schiavilla, and M. Viviani, Phys. Rev. C **87**, 014006 (2013).

[32] L.E. Marcucci, R. Schiavilla, and M. Viviani, Phys. Rev. Lett. **110**, 192503 (2013).

[33] M. Viviani, A. Baroni, L. Girlanda, A. Kievsky, L.E. Marcucci, and R. Schiavilla, Phys. Rev. C **89**, 064004 (2014).

[34] S. Ishikawa and M. R. Robilotta, Phys. Rev. C **76**, 014006 (2007).

[35] V. Bernard, E. Epelbaum, H. Krebs, and U.-G. Meissner, Phys. Rev. C **77**, 064004 (2008).

[36] V. Bernard, E. Epelbaum, H. Krebs, and U.-G. Meissner, Phys. Rev. C **84**, 054001 (2011).

[37] K. Hebeler *et al.*, arXiv:1502.02977.

[38] I. Tews, T. Krüger, K. Hebeler, and A. Schwenk, Phys. Rev. Lett. **110**, 032504 (2013).

[39] E. Epelbaum, Eur. Phys. J. A **34**, 197 (2007).

[40] D. Rozpedzik *et al.*, Acta Phys. Polon. B **37**, 2889 (2006).

[41] D.B. Kaplan, M.J. Savage, and M.B. Wise, Nucl. Phys. **B478**, 629 (1996); Phys. Lett. B **424**, 390 (1998); Nucl. Phys. **B534**, 329 (1998).

[42] See Refs. [146-164] in Ref. [20].

[43] A. Nogga, R.G.E. Timmermans, and U. van Kolck, Phys. Rev. C **72**, 054006 (2005).

[44] B. D. Day, Rev. Mod. Phys. **39**, 719 (1967).

[45] G. Baardsen *et al.*, Phys. Rev. C **88**, 054312 (2013).

[46] G. Hagen *et al.*, Phys. Rev. C **89**, 014319 (2014).

[47] H.Q. Song, M. Baldo, G. Giansiracusa, and U. Lombardo, Phys. Rev. Lett. **81** 1584 (1998).

[48] I. Bombaci and U. Lombardo, Phys. Rev. C **44**, 1892 (1991).

[49] D. Alonso and F. Sammarruca, Phys. Rev. C **67**, 054301 (2003).

[50] C. Drischler *et al.*, Phys. Rev. C **89**, 025806 (2014).